



# Vinculin E29R mutation changes cellular mechanics



Vera Auernheimer, Wolfgang H. Goldmann\*

Department of Physics, Biophysics Group, Friedrich-Alexander-University of Erlangen-Nuremberg, 91052 Erlangen, Germany

## ARTICLE INFO

### Article history:

Received 19 August 2014

Available online 1 September 2014

### Keywords:

Vinculin  
Talin  
F-actin  
Focal adhesion  
Mechanotransduction

## ABSTRACT

We investigated the effect of the point mutation E29R on vinculin under cell mechanical aspects. MEFvcl KO cells were transfected with intact eGFP-vinculin (rescue) or mutant E29R vinculin. Cellular stiffness and adhesion strength of mutant E29R vinculin were considerably higher compared to rescue and MEFvcl KO cells. 2D traction microscopy also indicated markedly higher strain energy in E29R mutant cells compared to rescue and MEFvcl KO cells. Fluorescence recovery after photobleaching showed that the recovery time for mutant E29R cells was drastically slower than for MEFvcl rescue cells and that the mobile fraction was larger for rescue compared to E29R mutant cells. These results indicate that E29R mutation might prime the vinculin head for F-actin binding, which results in higher cell stiffness, contractile force, and strengthening of focal adhesions.

© 2014 Elsevier Inc. All rights reserved.

## 1. Introduction

Vinculin is a globular focal adhesion (FA) protein consisting of 5 helical domains, where D1–D4 together form the vinculin head (Vh), which is connected to the vinculin tail domain (Vt) by a flexible linker region [1,2]. When the head domain (D1) interacts with the tail domain, the molecule is considered to be in a closed conformation. The tail domain contains binding sites for F-actin, paxillin, and PIP<sub>2</sub>, while the head domain, D1 holds binding sites for talin, alpha-actinin, and alpha-catenin. In the closed conformation, vinculin is unable to bind both filamentous actin at Vt and talin at D1. This conformation is also referred to as the auto-inhibited, inactive state. In the cytosol, vinculin adopts a default auto-inhibited conformation forming Vh and Vt intramolecular interactions.

Recently, Janssen et al. [3] proposed a model whereby F-actin binding to vinculin may weaken the interaction between the head and tail domain, which would increase the likelihood for talin (in cell–matrix interactions) or alpha-catenin (in cell–cell adhesions) to bind and fully activate vinculin [4]. According to these researchers, the D1 region of the vinculin head sterically clashes with F-actin that prevents the linkage between vinculin tail and F-actin.

Golji et al. [5] evaluated the impact of different vinculin head domain residues interacting with F-actin in molecular dynamics simulations. These researchers confirmed that D1 is separated from the vinculin tail in the open conformation, and found that the amino acids E28 and E29 are available for linking the vinculin head to the F-actin surface. They argued that the open conformation of

vinculin facilitates the binding of vinculin with F-actin not only by removing the steric hindrance for vinculin tail–F-actin interaction, but also through contributing an additional binding interface between D1 and F-actin. Alternatively, the clash between vinculin head (D1) and F-actin, if coupled with stress transduced to vinculin through its connection with talin, could also catalyze the movement of the head away from vinculin tail [5]. Conformational changes leading to the opening of the vinculin molecule have been described in several combinatorial models [2,6,7].

In this study, we analyzed vinculin's role using the MEFvcl E29R variant in magnetic tweezer, 2D–traction microscopic, and fluorescence recovery after photobleaching (FRAP) experiments and compared the results with MEFvcl rescue and MEFvcl KO cells. Our findings suggest that vinculin activation, F-actin binding, and subsequent force transmission are associated with amino acid E29 of vinculin as well as increased stability of vinculin incorporation in focal adhesions.

## 2. Materials and methods

### 2.1. Cell culture

Mouse embryonic fibroblasts (MEF) wild-type (WT) and vinculin knock-out (KO) were obtained from Dr. W.H. Ziegler [8]. These cell lines were maintained in a low glucose (1 g/L) Dulbecco's modified Eagle medium (Life Technologies, Darmstadt, Germany) supplemented with 10% fetal calf serum (low endotoxin) and 2 mM L-glutamine kept at 37 °C with 5% CO<sub>2</sub>. Mycoplasma contamination was excluded using a mycoplasma detection kit (Minerva Biolabs, Berlin, Germany).

\* Corresponding author.

E-mail address: [wgoldmann@biomed.uni-erlangen.de](mailto:wgoldmann@biomed.uni-erlangen.de) (W.H. Goldmann).

## 2.2. Cloning and expression of vinculin

Generation of the eukaryotic expression vector pcDNA3.1, including eGFP-tagged wild-type vinculin was previously described by [9]. The same cDNA vector was used to obtain the mutant. Using site-directed mutagenesis on position 29, glutamic acid (E) was replaced by arginine (R).

To create the point mutation, primers were ordered from MWG-Biotech (Eurofins MWG Operon, Ebersberg, Germany). Phusion High-Fidelity DNA Polymerase and the restriction enzyme DpnI for the digestion of methylated DNA were purchased from Cell Signaling (NEB, Frankfurt, Germany). DNA-vectors were amplified in *Escherichia coli* strain Dh5 $\alpha$  and purified using the NucleoBond PC 500 kit (Macherey–Nagel, Düren, Germany). The complete sequence for the eGFP-tagged vinculin mutant was confirmed by sequencing (GATC Biotech AG, Konstanz, Germany). MEF cells ( $1.5 \times 10^5$ ) were seeded overnight in 35 mm cell culture dishes prior to transfection. Transfection was carried out in serum-free DMEM using 2  $\mu$ g DNA and Lipofectamine 2000 (Invitrogen, Germany). The day after transfection, cells were re-seeded in 35 mm culture dishes or placed on PAA-traction gels, respectively.

## 2.3. Magnetic tweezer microrheology

We used a magnetic tweezer device as described by [10]. For measurements,  $3\text{--}4 \times 10^4$  cells were seeded overnight into a 35 mm tissue culture dish. Thirty minutes before the experiment, the cells were incubated with fibronectin-coated paramagnetic beads of 4.5  $\mu$ m  $\varnothing$  (Invitrogen, Karlsruhe, Germany). A magnetic field was generated using a solenoid with a needle-shaped core (HyMu80 alloy, Carpenter, Reading, PA). The needle tip was placed at a distance of 20–30  $\mu$ m from a bead bound to the cell using a motorized micromanipulator (Injectman NI-2, Eppendorf, Hamburg, Germany). A staircase-like, increasing force was then applied for 10 s to the bead bound on the cell surface [11]. During measurements, bright-field images were taken by a CCD camera (ORCA ER, Hamamatsu) at a rate of 40 frames/s. The bead position was tracked on-line using an intensity-weighted center-of-mass algorithm. Measurements on multiple beads per well were performed at 37  $^\circ$ C for 0.5 h, using a heated microscope stage on an inverted microscope at 40 $\times$  magnification (NA 0.6) under bright-field

illumination. Transfected eGFP-positive MEF cells were identified in fluorescence mode.

## 2.4. 2D-traction microscopy

Different MEFs were plated overnight on fibronectin-coated polyacrylamide hydrogels (Young's modulus of 18,000 Pa) at 37  $^\circ$ C and 5% CO $_2$  in DMEM medium. Gels were prepared according to a modified protocol by Pelham and Wang [12]. Using cytochalasin D and trypsin, cells were detached and images were recorded before and after relaxation of the gel. Comparing the position of fluorescent microspheres in the deformed and undeformed states, the traction field was obtained using a difference-with-interpolation algorithm with a spatial resolution of 2.5 nm and an accuracy of 8 nm. Traction fields were computed according to a Fourier-based-algorithm [13].

## 2.5. Fluorescence recovery after photobleaching (FRAP)

FRAP studies were performed with the confocal microscope (Leica) and a 20 $\times$  dip-in objective inside the incubation chamber. Transfected cells were cultivated in 35 mm dishes the day before, and cells – expressing medium levels of eGFP-vinculin constructs and focal adhesions that showed no growth or disassembly – were chosen for measurements. A 488 nm argon laser was used for eGFP excitation and bleaching. Image acquisition started 1 min before bleaching and continued for 5 min of the recovery process (1 frame/4 s). FRAP movies were analyzed using ImageJ and Matlab software [14]. Intensities of the bleached focal adhesions as well as reference adhesions were corrected for background fluorescence, and the bleached area was normalized by the average reference adhesion signal. Every recovery curve was fitted with a single exponential function, and the mean value of all half-life recovery times ( $t_{1/2}$ ) as well as the immobile fractions were calculated.

## 3. Results and discussion

Glutamic acid (E, negatively charged) on position 29 of the vinculin molecule was replaced by arginine (R, positively charged) to test the cellular mechanical changes induced by this point mutation. Both vinculin constructs, (full length vinculin = rescue) and

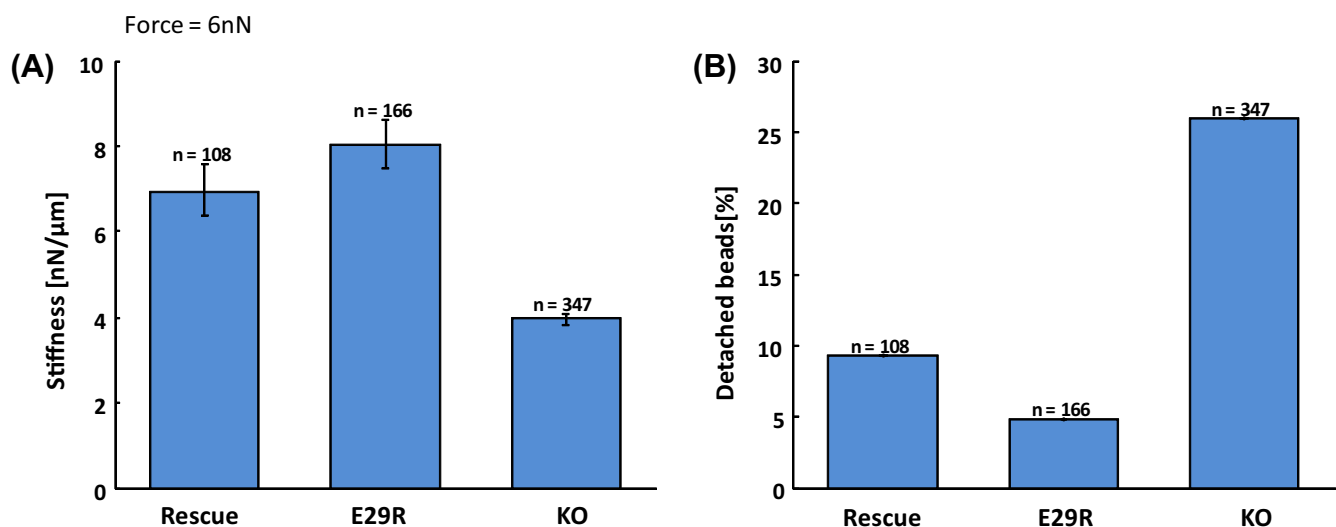


**Fig. 1.** (A) Magnetic tweezer measurements of MEFvcl rescue, MEFvcl E29R, and MEFvcl KO cells. All cells were incubated with fibronectin-coated paramagnetic beads ( $\varnothing$  4.5  $\mu$ m) for 30 min, after which the paramagnetic beads were displaced from their original position by force application of the magnetic tweezer. From the displacement, the cell stiffness was calculated at 6 nN force. The standard error of the mean (SEM) and the number of cells are indicated. (B) Binding (adhesion) strength of MEFvcl rescue, MEFvcl E29R, and MEFvcl KO cells are represented by the percentage of detached beads during measurements.

Download English Version:

<https://daneshyari.com/en/article/10753835>

Download Persian Version:

<https://daneshyari.com/article/10753835>

[Daneshyari.com](https://daneshyari.com)